

## SUPPLEMENTAL MATERIAL

### Supplemental Methods

The VMAP (Vectorcardiographic Mapping of Arrhythmogenic Probability) study was a blinded, multicenter clinical study with final data analysis performed by an independent core laboratory (Cardiovascular Research Foundation, New York, NY) to validate the performance of a computational ECG mapping system. The study protocol was reviewed and approved by governing Institutional Review Boards (IRBs) at all sites and was conducted in accordance with all applicable human subject research requirements and applicable federal regulations. It was registered on ClinicalTrials.gov (NCT04559061) on September 22, 2020.

#### **Study Design**

The study was designed as a blinded, multi-center clinical study with data analysis performed by an independent core laboratory.

#### **Data Collection and Study Phases**

The clinically indicated electrophysiology study was conducted prior to study activation at each clinical site. The clinical procedure was conducted according to physician preference, including standard-of-care arrhythmia entrainment/induction, activation mapping, pace mapping, and/or phase analysis to localize the arrhythmia source or sources. Surface ECG electrodes were placed per clinical electrophysiology laboratory protocol at participating centers; no specific guidance or restrictions on ECG lead placement were specified by the VMAP study protocol. The study consisted of 4 phases: A-D.

##### *Phase A: Case Identification and Eligibility*

Eligible cases were identified from extant medical records at participating institutions. To minimize selection bias, cases were reviewed and enrolled consecutively in reverse chronological order based on the date of the ablation procedure, starting from the date of official site activation. To methodically operationalize the case identification process, a Case Identification Log was used to document screening and enrollment information including the result of the case screening.

- Upon documented case eligibility, the case was assigned a unique identification code and de-identified. Case information and disease characteristics data were entered in the study database.
- Case information included subject demographics: sex, age range, weight, height, BMI (automatically generated by study database), ejection fraction, NYHA heart failure classification, disease substrate type (e.g., ischemic cardiomyopathy), and amiodarone use.
- If the patient's ECG or arrhythmia/pacing type were unavailable or of insufficient quality, the case was not considered eligible.

##### *Phase B: Arrhythmia Source or Pacing Site “Gold Standard” Localization*

The electrophysiologist from the data-originating site (EP#1) identified the 12-lead ECG recorded during the induced arrhythmia, downloaded de-identified digitized ECG data from the

electrocardiographic recording system to secure media, and annotated/marked the time period of interest containing the arrhythmia on the digitized ECG. EP#1 then marked the location of the arrhythmia source or pacing site, based upon the location(s) of successful ablation or pacing during invasive electrophysiology study, onto a 3-dimensional model of the heart using a single reference geometry provided to all EPs to define cardiac regions and segments.

EP#1 then recorded the chamber/region and segment (based on pre-defined, published atrial<sup>12</sup> and ventricular<sup>13</sup> segmentation models, see below) of the arrhythmia source or pacing site location into the 21 CFR Part 11-compliant electronic data capture system (CliniOps, Fremont CA). The arrhythmia source or pacing site location determined by invasive electrophysiology study was considered the “gold standard” for accuracy determination. Data supporting the reference standard (e.g., images from electroanatomic mapping, fluoroscopy, etc.) were optionally uploaded to the electronic data capture system as well. These data and evidence were only accessible to the Core Laboratory, not to EP#2 (who remained blinded to these results). If the case was associated with multiple arrhythmia/pacing episodes, the steps were repeated for each episode. Completed arrhythmia/pacing episodes were then ‘promoted’ to EP#2 to utilize the ECG mapping software in Phase C.

#### *Phase C: Mapping Algorithm Processing*

Once cases were ‘promoted’ to phase C, they were assigned to an independent, blinded EP#2 (to a study investigator who was not the case originator and had no knowledge of the episode ground truth). For each case, the EP#2 referenced the CliniOps study database and manually populated the necessary case information and disease characteristics into the mapping software. EP#2 employed the mapping software in accordance with the Instructions for Use to generate the system output. The system output (i.e., the output ‘map’ presented on the cardiac model identifying mapping hotspot(s) based on chamber/region and cardiac segment) was then transferred to a USB drive and upload to the electronic data capture system. Completed cases were then ‘promoted’ to the Core Lab for endpoint analysis (phase D).

#### *Phase D: Core Lab Endpoint Analysis*

Cardiovascular Research Foundation (CRF, New York, NY, USA; “Core Laboratory”) analyzed the results in accordance with study protocol-prescribed study endpoints, with the exception of the spatial accuracy analysis, which was completed by automated software without the need for manual data analysis or entry.

In accordance with the Manual of Operations, the Core Lab reviewed the case/episode data made available to them via the study database, including:

- The arrhythmia source or pacing site location (“gold standard”): chamber/region and segment(s) that were reported directly in the EDC system by EP#1. The 3D heart image with indicated ground truth source location as well as spreadsheet notations of source/site heart chamber/region and segment(s) were also available as confirmatory materials.
- ECG mapping software hotspot: algorithm output that was generated separately by EP#2, which included the algorithm-generated hotspot segment(s).

The Core Lab reported agreement/non-agreement results directly into the study EDC database. The Core Lab also reported the segment number(s) listed on the mapping system output PDF in the study database. The analysis process was repeated for each arrhythmia/pacing episode.

## **Cardiac Segmentation Models**

Cardiac Segments were pre-defined for the study based upon prior work as shown below.

### *Atrial Segments*

A total of 21 atrial segments were pre-defined based on prior work by Sohns and colleagues<sup>12</sup> as shown in **Supplemental Figure I**.

### *Ventricular Segments*

There were 30 ventricular segments derived from prior work by Plaisier and colleagues<sup>13</sup> as shown in **Supplemental Figure II**.

## **Device Description**

The ECG mapping system (e.g., “algorithm” or “software”) is a non-invasive tool for mapping the sources of cardiac arrhythmias and pacing within the atria and ventricles. It displays ECG signals, signal analysis results, and 3-dimensional maps.

It receives 12-lead ECG signals acquired from the body surface. The ECG signals are then analyzed using forward-solution approach which involves comparison of patient ECG with the data contained within a library of cardiac arrhythmia simulations (currently >1 million arrhythmia cycles). Optionally, data regarding patient demographics and patient physiology/pathophysiology may be entered using a menu-driven interface to enhance patient specificity.

The algorithm then transforms the ECG data into 2D cardiac information and interactive 3D color maps for analysis by a physician. It can be used in the clinical environment, such as the electrophysiology (“EP”) lab and at the patient’s bedside. Please see section III (below) for additional mapping algorithm details.

## **Study Population**

Cases inclusion criteria enrolled patients reflecting the spectrum of patients commonly treated in the clinical electrophysiology setting.

### *Inclusion Criteria*

1. Patient had one of the 9 following types of clinical arrhythmia/pacing:
  - Premature atrial complexes
  - Focal atrial tachycardia
  - Atrial pacing
  - Atrial fibrillation
  - Orthodromic atrioventricular reentrant tachycardia
  - Premature ventricular complexes
  - Ventricular tachycardia
  - Ventricular pacing
  - Ventricular fibrillation
2. Patient had undergone ‘successful’ routine, standard of care diagnostic electrophysiology (EP) study using intracardiac catheters as clinically indicated, guided by fluoroscopy and routine electroanatomic mapping, intracardiac echocardiography, and/or cardiac imaging such as CT or MRI.

3. 12-lead electrogram data of clinical rhythms (including baseline, pacing, and clinical arrhythmia) was recorded on the electrogram recording system (Bard, Boston-Scientific; Prucka, GE Medical; or Workmate Claris, Abbott) or stand-alone ECG system (e.g., CardioCard, Nasiff Associates, Brewerton, NY) in digitized format.
4. Patient had undergone ‘successful’ ablation procedure with targeted therapy, defined as: 1) inability to induce arrhythmia after the ablation; or 2) clinical freedom from arrhythmia at 6 months.
5. The following data elements were able to be abstracted from the patient medical records (to be entered into the ECG mapping system):
  - Arrhythmia type;
  - Atrial characteristics: geometry (normal, left and/or right atrial enlargement), Utah classification (if available), prior ablation, and ablation type; and
  - Ventricular characteristics: ventricular geometry (normal, left and/or right ventricular dilation), scar location(s).
6. Patient was between 22 and 100 years of age at time of EP study and ablation procedure.

#### *Exclusion Criteria*

Exclusion criteria consisted of the following:

- Patients with unstable coronary artery disease.
- Patients with presence of confirmed intracardiac thrombus in the chamber of interest.
- Patients with active sepsis at the time of his/her ablation procedure.
- Patients with complex congenital heart disease.
- Patients with dextrocardia.
- Patients with severe pulmonary hypertension.
- Patients with decompensated heart failure.
- Patients with an existing mechanical heart valve.
- Patients who experienced myocardial infarction within 1 month of his/her ablation procedure.
- Inability to induce the clinical rhythm or arrhythmia.
- Unacceptable ECG data quality including low ECG signal-to-noise ratio.
- The patient dataset was included as a sample for validating the ECG mapping algorithm (Table S2, below).

#### *Case Selection*

To minimize selection bias, cases were reviewed and identified consecutively in reverse chronological order based on the date of the ablation procedure, starting from the date of official site activation. Thus the ‘start’ date was different for each clinical site and was predicated on site activation. Sites ceased data collection once they reached their prespecified targeted number of cases or upon notification by the Sponsor based on the remaining arrhythmia/pacing types needed for analysis.

Upon documented case eligibility (refer to Inclusion Criteria and Exclusion Criteria), the case was assigned a unique identification code: the two-digit number assigned to the site, followed by a three-digit case number (e.g., 01-001) assigned consecutively.

To methodically operationalize the case identification process, a Case Identification Log was used to document screening and enrollment information.

#### *Protocol Details: Atrial Fibrillation Mapping and Ablation*

The methodology used for inducing, mapping, and ablating AF for patients included in the VMAP study is detailed separately<sup>28</sup>. In summary, spontaneous or induced AF was recorded using 64-electrode basket catheters. AF recordings were analyzed using activation and phase analysis to localize sites of wavefront slowing and curvature. The most stable 3 to 4 sites were then targeted with ablation. Following targeted AF electrical substrate ablation, attempts were made to re-induce AF with pacing per protocol.

As specified by the study inclusion criteria, all enrolled AF patients were either (a) non-inducible at the conclusion of the protocol or (b) arrhythmia free for a minimum of 6 months after ablation. The ablation site or sites targeted during the procedure were considered the “gold standard” for this study.

#### *Protocol Details: Ventricular Fibrillation Mapping and Ablation*

The methodology used for inducing, mapping, and ablating VF for patients included in the VMAP study is documented in prior work<sup>29</sup>. Briefly, VF was induced with protocol-directed extrastimulus or burst pacing. Endocardial activation during VF was recorded using bi-ventricular 64-electrode basket catheters. VF recordings were analyzed using activation and phase analysis to localize sites of wavefront slowing and curvature. The most stable 3 to 4 VF electrical substrate sources were then ablated. VF-triggering PVCs and VT were not enrolled as VF sources in the VMAP study. Following ablation, attempts were made to re-induce VF with the same protocol as pre-ablation.

As specified by the study inclusion criteria, all enrolled VF patients were either (a) non-inducible at the conclusion of the protocol or (b) arrhythmia free for a minimum of 6 months after ablation. The ablation site or sites identified by this process were considered the “gold standard” for this study.

## **Study Endpoints**

### *Endpoint Planning and Analysis*

In this study, the primary and secondary endpoints were endpoints for which detailed power calculations were performed and the study was statistically powered to assess. Additionally, the primary and secondary endpoints were associated with a statistical P value compared with pre-specified performance goals.

Ancillary endpoints had enrollment targets and analyses were enabled if all primary and secondary endpoint analyses rejected the study null hypothesis. Unlike the primary and secondary endpoints, ancillary endpoints were not compared against a pre-specified performance goal. Post-hoc analyses were performed to further assess specific areas of algorithm performance.

### *Primary Endpoint*

The primary effectiveness endpoint was defined, based upon prior seminal work<sup>17</sup>, as accuracy of the ECG mapping algorithm in correctly identifying the ventricular chamber/region of the arrhythmia source or pacing site location based on diagnostic information determined during the invasive EP study and ablation (known as the “gold standard”) for premature ventricular complex (PVC) and ventricular tachycardia (VT) arrhythmia types in cases with structurally normal hearts and less than 10% scar.

Accuracy (successful localization) was defined as:

- The mapping hotspot output result from the ECG mapping algorithm is within the identified ventricular chamber/region of the heart as determined by the gold standard from electrophysiology study and ablation.
- The ventricular chamber/region is defined as the following: left ventricular free wall, septum, or right ventricular free wall.

### *Secondary Endpoints*

The secondary endpoints were defined as the following:

1. Secondary endpoint 1 was defined as the accuracy of the ECG mapping algorithm in correctly identifying the chamber/region<sup>17</sup> of the arrhythmia source or pacing site compared with diagnostic information determined during the invasive EP study and ablation (known as the “gold standard”) across all arrhythmia/pacing types, including cases with structurally abnormal hearts and greater than 10% scar.

Accuracy (successful localization) was defined as:

- The mapping hotspot output result from the ECG mapping algorithm was within the identified chamber/region of the heart as determined by the gold standard.
- The chambers/regions were defined as the following:
  - Atria: left atrial free wall, septum, or right atrial free wall; and
  - Ventricles: left ventricular free wall, septum, or right ventricular free wall.

2. Secondary endpoint 2 was defined, based upon prior elegant work<sup>2, 25</sup>, as the accuracy of the ECG mapping algorithm in correctly identifying the precise or neighboring segment of the arrhythmia source or pacing site location compared with diagnostic information determined during the invasive EP study and ablation (known as the “gold standard”) across all arrhythmia/pacing types, including cases with structurally abnormal hearts and greater than 10% scar

Accuracy (successful localization) was defined as:

- The mapping hotspot location as identified by the ECG mapping algorithm is within the identified segment or an adjacent segment of the 21 atrial segment model (based upon work by Sohns et al.<sup>12</sup>) or 30 ventricular segment model (based upon work by Plaisier et al.<sup>13</sup>) compared with the gold standard location determined by electrophysiology study and ablation.

### *Ancillary Endpoints*

Ancillary endpoints 1 and 2 were defined as the mapping algorithm regional and segmental accuracy, respectively, for each of the 9 arrhythmia or pacing types individually. Ancillary endpoint 3 was defined as the time interval (in minutes) between upload of the digitized ECG into the mapping software and display of the 3-dimensional mapping result.

## Statistical Methods, Performance Goals, and Sample Size Calculations

### *Primary Endpoint: Performance Goal and Hierarchical Testing*

For the primary endpoint, the pre-specified performance goal was that the lower boundary of the 95% confidence interval equal or exceed 80% for PVCs and VT in patients without significant structural heart disease, based upon prior seminal work<sup>2, 17, 30</sup>. Thus, the null hypothesis for this endpoint is a one-sided ( $\alpha=0.025$ ) t-test of  $H_0<0.8$ , and the alternative hypothesis is  $H_a\geq 0.8$ . This performance goal is based upon an expected accuracy for this metric of approximately 95% from pre-study validation testing in a separate validation group.

If the primary endpoint success criterion is met, the secondary endpoints will be tested in order, stopping if a test fails to reject the null hypothesis at  $\alpha=0.025$ . This hierarchical testing algorithm preserves study alpha at 0.025.

### *Secondary Endpoints Analysis*

For secondary endpoint 1, the pre-specified performance goal was that the lower boundary of the 95% confidence interval equal or exceed 75% based upon prior work<sup>5, 18</sup>. Thus, the null hypothesis for accuracy for secondary endpoint 1 is  $H_0<0.75$ , and the alternative hypothesis is  $H_a\geq 0.75$ . This performance goal is based upon an expected accuracy for this metric of approximately 83% based upon pre-study validation testing.

For secondary endpoint 2, the pre-specified performance goal was that the lower boundary of the 95% confidence interval equal or exceed 70%, based upon prior work<sup>19</sup>. Thus, the null hypothesis for accuracy for secondary endpoint 2 is  $H_0<0.70$ , and the alternative hypothesis is  $H_a\geq 0.70$ . This performance goal is based upon an expected accuracy for this metric of approximately 79% based upon pre-study validation testing.

### *Ancillary Endpoints Analysis*

If all primary and secondary analyses rejected the null hypothesis, ancillary endpoint analyses were enabled. Ancillary endpoints 1 and 2 were determined as the mapping algorithm regional and segmental accuracy with associated 95% confidence intervals. The third ancillary endpoint, workflow efficiency, was measured in minutes and presented as median, 25%, and 75%iles.

### *Power Calculations and Determination of Sample Size*

For the primary endpoint, based on the expectation of 95% accuracy (derived from pre-study validation data separate from this study population) of correctly identifying the region of interest, 60 evaluable PVC/VT arrhythmia datasets were required for a 90% power at a 1-sided alpha of 0.025 to reject the null hypothesis ( $H_0$ ) that the true accuracy is less than 80% ( $H_0<0.8$ ). The alternative hypothesis was that the true accuracy is greater than or equal to 80% ( $H_a\geq 0.8$ ).

For secondary endpoint 1, based on the expectation of 83% accuracy of correctly identifying the region of interest, a minimum of 250 evaluable patient arrhythmia/pacing datasets were required for an 85% power at a 1-sided alpha of 0.025, to reject the null hypothesis that the true accuracy is less than 75% ( $H_0<0.75$ ). The alternative hypothesis is that the true accuracy is greater than or equal to 75% ( $H_a\geq 0.75$ ).

For secondary endpoint 2, based on the expectation of 79% accuracy of correctly identifying the precise or neighboring segment of interest, a minimum of 250 evaluable patient arrhythmia/pacing datasets were required for an 89% power at a 1-sided alpha of 0.025, to reject

the null hypothesis that the true accuracy is less than 70% ( $H_0 < 0.70$ ). The alternative hypothesis is that the true accuracy is greater than or equal to 70% ( $H_a \geq 0.70$ ).

All arrhythmia/pacing types were to include no less than 20 samples and no more than 30 samples to accommodate ancillary endpoints 1 and 2, with exception of PVCs and VTs whose enrollments could be greater to accommodate the analysis populations for both the primary endpoint (structurally normal hearts and <10% scar) and secondary endpoints (including structurally abnormal hearts and >10% scar).

Assuming a 10% attrition rate due to screen failures following database entry (e.g., poor signal-to-noise on ECG), up to 25 additional patient arrhythmia/pacing datasets could be evaluated to meet or exceed enrollment goals.

## **Sources of Error and Approaches to Mitigate Error**

### *Spatial Analysis: Error Inherent to Boundary Problems*

Assessment of segmental accuracy is a boundary problem in spatial analysis<sup>31</sup> and may be subject to several types of error. Among these is edge effect<sup>31</sup>, which introduces significant potential uncertainty in assessing the performance of a given system.

Given the expected algorithm mapping performance from validation work, we clustered exact plus neighboring segments to help mitigate edge effect bias as recommended by prior work in spatial analysis<sup>32</sup> to reduce the risk of type II error in the secondary and ancillary endpoints. Post-hoc exact segment accuracies for all episodes and for selected sub-populations based upon prior work<sup>25</sup> are also reported.

### *Site Transposition Spatial Error*

Transposition of spatial locations by an electrophysiologist from one 3-dimensional computational cardiac model to another in order to define the study “gold standard” site was identified as a potential source of error. The magnitude of the transposition error was assessed prior to initiation of the clinical study using the following methodology.

In summary, electroanatomic mapping data from 3 successful ablation cases (1 PVC, 1 VT, and 1 focal AT, separate from the patients in the clinical study) was shown to 3 blinded electrophysiologists (from the pool of GH, KSH, FR, FTH). The electrophysiologists annotated the location of the site of ablation on a 3-dimensional computational cardiac geometry without mapping details (e.g., no voltage or activation information).

These marks were then compared to the location of the “gold standard” site of successful ablation. The spatial error was quantified using the distance measurement tools in the electroanatomic mapping software (Carto, Biosense-Webster, Irvine, CA, USA). The mean and standard deviation spatial error in this transposition process were  $5 \pm 3$  mm.

To minimize transposition error, study investigators were required to complete study training including a suite of practice cases prior to enrolling patients in the VMAP study.

## **Mapping Algorithm Description**

### *Mapping Algorithm Overview*

The mapping algorithm performs non-invasive, beat-by-beat, multi-chamber mapping of atrial and ventricular arrhythmias and pacing by utilizing a forward-solution strategy comparing electrogram data from the patient and a pre-computed library of arrhythmia simulations. Matches between patient data and relevant simulation samples are used to compose heatmaps of potential



arrhythmia source or pacing site locations. The feature mapped for each arrhythmia and pacing type is noted in **Supplemental Table I**.

#### *Computational Arrhythmia Simulation Library*

The arrhythmia simulation library currently consists of >1 million simulations of cardiac electrical activity in finite element models of electrophysiology with arrhythmia and pacing locations as input parameters as illustrated in **Supplemental Figure III**. This database serves as the algorithm “learning set” which was created and “locked” prior to study initiation; no changes to the simulation library were permitted during the VMAP study.

#### *Forward Solution Implementation and Data Flow*

The mapping process and forward solution approach are illustrated in **Supplemental Figure IV**. The process begins with upload of 12-lead ECG data into the system using an interactive user interface (1). Details regarding the presence or absence of structural heart disease, fibrosis, chamber hypertrophy, chamber dilation, and other characteristics are entered into the system using a drop-down menu system. These data are then passed to the mapping algorithm (2), which selects the most appropriate simulations for comparison from the pre-computed simulation library (3) based upon user inputs.

Within the algorithm, electrogram data is processed according to the following steps. First, activation patterns are estimated using vectorcardiograms (VCGs) derived from standard 12 lead ECGs using inverse Dower and Kors transformations<sup>10</sup>. Next, differences between measured and computed VCGs were minimized to identify the most relevant arrhythmia simulations. The algorithm evaluates each chamber’s electrical activation as an integrated event which is compared to the integrated activation event from the relevant cardiac simulations.

Simulations corresponding to the highest ranked matches are then identified. The locations of the initial conditions which initiated or sustained the simulated arrhythmia are then returned to the mapping algorithm. The locations of these sites are processed and plotted on the 3-D output as high-probability regions of arrhythmia source locations. Heatmap colors illustrate the spectrum from higher probability sites to lower probability sites.

#### *Finite Element Models of Cardiac Electrophysiology*

The cardiac arrhythmia simulation library is based on finite element models of cardiac electrophysiology. The models simulate electrical activation initiated from specified locations in the heart. The models were formulated and simulated using the *Continuity*<sup>10, 11, 16, 33</sup> environment developed by the Cardiac Mechanics Research Group led by Dr. Andrew McCulloch at the University of California San Diego. The models consist of mathematical descriptions of cardiac geometry, myofiber orientation, disease substrate, transmembrane current flow, and myocardial conduction. *Continuity* is distributed free for academic research by the National Biomedical Computation Resource.

#### *Governing Equations: Cardiac Action Potential Propagation*

Cardiac action potential propagation in the heart is modeled according to the monodomain equation. It is a reaction-diffusion system based on conservation of ionic currents in the cardiac domain, with the assumption that currents between the two domains are proportional. The monodomain equation is given by:

$$\chi \left( C_m \frac{\partial V}{\partial t} + I_{ion}(V) \right) = \nabla \cdot \sigma \nabla V \quad \text{Equation 1}$$

where  $V$  is the myocyte transmembrane potential (mV),  $\sigma$  is the conductivity tensor ( $\text{mS} \cdot \text{mm}^{-1}$ ),  $C_m$  is the specific capacitance of the cell membrane ( $\mu\text{F} \cdot \text{mm}^{-2}$ ), and  $\chi$  ( $\text{mm}^{-1}$ ) is the surface-area-to-volume ratio of the myocyte.  $I_{ion}$  ( $\mu\text{A} \cdot \text{mm}^{-2}$ ) is the electrical current density due to the flow of ions through channels embedded in the cardiomyocyte cell membrane. The gating dynamics of the ion channels are modeled by a function  $f$  that depends on the transmembrane potential  $V$ , time  $t$ , and a set of state variables  $y$  that represent ion channel states:

$$I_{ion} = f(y, t, V) \quad \text{Equation 2}$$

The state variables in  $y$  are governed by a set of nonlinear ordinary differential equations  $g$ :

$$\frac{dy}{dt} = g(y, t, V), \quad \text{Equation 3}$$

which determine the time rates of change of ion channel state variables. The particular equations for  $I_{ion}$  and  $\frac{dy}{dt}$  are described by ionic current models constructed for particular kinds of cardiomyocytes (atrial vs. ventricular) and electrophysiologic properties (healthy vs. diseased). Together, these ordinary differential equations (ODEs) make up the reaction component of the monodomain equation. The diffusion component is made up of the partial differential equation (PDE) on the right-hand side which models the passive spread of action potential currents in myocardial tissue. Finally, a boundary condition of zero current flux across the surfaces of the geometric domain is applied:

$$n \cdot (\sigma \nabla V) = 0 \quad \text{Equation 4}$$

where  $n$  is the outward-pointing normal unit vector at a point on the boundary.

### *Model Configurations, Properties, and Conditions*

The finite element models which produced the arrhythmia simulation library were carefully chosen to represent the spectrum of phenotypes and arrhythmia mechanisms commonly seen in the clinical cardiac electrophysiology setting. Finite element modeling methods have been described in detail in previously published work<sup>10, 15</sup>. We briefly review the modeling configurations, properties, and conditions in the following sections.

#### *Cardiac Geometry*

Patients with atrial and ventricular arrhythmias present with a range of structurally normal and abnormal chamber geometries<sup>34, 35</sup>. The user can select, via a menu-driven input process, the most relevant structural phenotype for the atrial or ventricular arrhythmia of interest. The selected phenotype is then mapped to simulations within the arrhythmia library most relevant to the clinical patient.

#### *Myofiber Architectures*

Bi-ventricular fiber architectures in the ventricular meshes are based empirically on diffusion tensor (DT) MRI measurements of a human cadaver heart<sup>14,33</sup>. Bi-atrial fiber architectures in atrial meshes use a rule-based definition of atrial myocyte fiber angles based on typical measurements from explanted human atria<sup>36</sup>.

#### *Myocardial Scar, Fibrosis, and Prior Ablation Lesions*

In patients, the presence of scar, fibrosis, and existing surgical or ablation lesions may impact the global cardiac activation pattern. A user may select from one of several common scar locations, degrees of fibrosis, and ablation lesion patterns for atrial and ventricular arrhythmia episode types. The selected phenotypes are mapped to arrhythmia simulation libraries based on models with the selected scar, fibrosis, or ablation lesion phenotype.

#### *Ventricular Scarring*

Clinically, large regional scars (greater than or equal to approximately 10% of ventricular myocardium) may significantly impact patient cardiac electrophysiology<sup>37,38</sup>; To account for this, 4 primary regions of left ventricular scar were created in the simulation library, with scars located in the LV anterior, lateral, inferior, and septal walls. Combinations of up to 3 scar regions may be selected by the user using a menu-driven interface for mapping.

#### *Atrial Fibrosis*

Patients with atrial arrhythmias often present with some degree of atrial fibrosis. The extent of fibrosis is classified according to Utah stages<sup>39</sup>, which is based on the percent of fibrotic atrial mass as measured by delayed enhancement MRI. Users may optionally select Utah stage I through IV from a menu-drive interface during analysis.

#### *Ablation Patterns*

Patients with recurring atrial arrhythmias such as persistent atrial fibrillation often present with lesions from one or more prior ablation procedures<sup>40</sup>. Using a similar approach as ventricular scar, we modeled 5 types of common ablation lesion patterns,<sup>41,42</sup> which may be selected during mapping. These common ablation patterns include pulmonary vein isolation, LA roof linear ablation, anterior mitral isthmus linear ablation, posterior mitral isthmus linear ablation, and cavotricuspid isthmus ablation. Users may select from these ablation patterns via menu choices during mapping.

#### *Arrhythmia Source Mechanisms and Locations*

The mapping software accounts for two types of arrhythmia source mechanisms: focal activation and unstable spiral wave-reentry (electrical rotor) activation patterns and described in detail below.

#### *Focal Arrhythmias*

Arrhythmias whose cardiac activation pattern may be approximated by simulations of focal electrical activation include premature atrial and ventricular complexes<sup>22</sup>, focal atrial tachycardia, some forms of ventricular tachycardia<sup>22</sup> (excluding polymorphic VT), atrial<sup>26</sup> and ventricular pacing<sup>26</sup>, and atrial activation during orthodromic atrioventricular reentrant tachycardia. Representative simulations were created by applying point stimulus currents in the models.

### *Unstable Spiral Wave Reentry (Electrical Rotor) Arrhythmias*

Arrhythmias in which ongoing activation which may be approximated by simulations of spiral wave functional reentry (electrical rotors) include atrial<sup>6, 8, 28</sup> and ventricular fibrillation<sup>9, 29, 43, 44</sup>. Such analysis is best suited to determine the site or sites which sustain the arrhythmia after initiation<sup>28, 29</sup>; focal triggers which initiate AF or VF may be mapped using focal analyses (described above).

### *Ionic Current Models of Ventricular and Atrial Myocytes*

Myocardial cell ionic currents (the  $I_{ion}$  term in monodomain Equation 1) were based on published models and parameters for ventricular and atrial myocytes. We used the human ventricular-based Ten Tusscher et al.<sup>45</sup> cell model for ventricular arrhythmia simulations. We used a model of atrial myocytes based on work by Koivumäki et al.<sup>46</sup> for atrial arrhythmias.

### *Processing Arrhythmia Simulations*

The simulation samples were catalogued by characteristics noted above. Presently, the library consists of more than 1 million arrhythmia cycle simulations from the 418,500 model variations created to accommodate variations in anatomy, physiology, and pathophysiology.

### *User Interface*

The mapping system provides a graphical interface to input patient information, load ECG data for analysis, and evaluate mapping results. It allows selection of an ECG tracing of interest and designation of a sub-segment of the digital ECG data for mapping. Patient characteristics input into the system are used to select the most relevant arrhythmia simulation subset for the mapping process.

After mapping, the interface allows users to select the appropriate cardiac surface or surfaces for heatmap display, and to rotate, pan, and magnify the image for viewing and interpretation.

### **Algorithm Verification**

The *Continuity* simulation environment has been previously verified<sup>15</sup> against a well-known community benchmark problem originally posed by Niederer et al<sup>47</sup>. The results demonstrated excellent agreement between *Continuity* and the consensus solution, supporting proper implementation of numerical modeling methods.

### **Algorithm Clinical Validation**

In prior work<sup>10</sup>, the electrical activation patterns produced by the models demonstrated good agreement in with clinical ventricular activation time as assessed by invasive electroanatomic mapping.

In an AF model, simulations of wavefront propagation in atria with extensive electrical remodeling demonstrated wavebreak and the initiation of AF consistent with clinical observations<sup>8</sup>.

In other work<sup>9</sup>, simulated and clinical VF were compared. The computational models exhibited complex behavior including wavebreak and simultaneous rotors, which were clinically observed in patients with clinical VF. Additionally, beat-to-beat rotor meander on the order of

1.5 cm was observed clinically patients and in VF simulations. Finally, in both patients and simulations, VF exhibited significant surface ECG amplitude variation.

In proof-of-concept work, 6 patients with refractory ventricular tachycardia were mapped. Stereotactic ablative radiotherapy was targeted at VT substrate sites and a significant reduction in VT events was noted<sup>1</sup>.

### **Results in a Clinical Validation Set**

Results from a validation set, completed prior to the initiation of the VMAP study and separate from the enrolled study patients, were used to (1) determine when the number of simulations was adequate to represent study arrhythmias and pacing and (2) statistically power the VMAP study. The validation set was analyzed according to the episode-specific disease characteristics as shown in Supplemental Table II and scored against the cardiac region and segment of the gold standard site of EP study-determined pacing site or arrhythmia source location. Regional and segmental accuracy were measured as defined in “Study Endpoints” (above).

## **Supplemental Results**

### **Primary Endpoint Accuracy According to Study Center**

We analyzed the primary endpoint results according to study center of origin. The results of this analysis are shown below in **Supplemental Table III**, below. In summary, accuracy for the primary endpoint was not significantly different among study sites ( $p=0.08$ ).

### **Spatial Accuracy Analysis: Additional Images and Data**

**Supplemental Figure V** illustrates the voltage map created during VT ablation corresponding to the clinical study patient illustrated in manuscript Figure 2, second row. The patient experienced a myocardial infarction 24 years prior to study enrollment and dual chamber ICD implantation 12 years prior. Nuclear sestamibi imaging before the ablation procedure showed an extensive, transmural filling defect of the inferior/posterior wall extending to the apex and an ejection fraction of 38%. No reversible filling defects were noted.

During noninvasive ECG mapping, the “LV posterior scar” option was selected from the drop-down menu. The mapping results demonstrated a spatial accuracy (center-to-center absolute distance between the successful ablation site and mapping output) of 5 mm. The patient remains free of VT and ICD shocks at 12 months follow-up.

### **Modeled versus Patient-Specific Spatial Accuracy Substudy**

To assess the agreement between spatial accuracy using the standard model (as performed in the study) and patient-specific spatial accuracy, we created 3-dimensional reconstructions of the atrial and ventricular anatomies for 10 randomly selected study patients. In blinded analysis, the location of the gold-standard site of ablation was tagged on the patient-specific anatomy with a 3-dimensional marker. Separately, and in blinded fashion, the site corresponding to the output of the mapping system was tagged on the patient-specific anatomy. The two sets of markings were then combined onto a single geometry and the spatial distance between the two markings was measured using DICOM viewing software (Horos, Horos Project, Annapolis, MD, USA).

We then compared the spatial error determined the patient-specific error with the error as estimated using the standard model as shown in **Supplemental Figure VI**. The actual and estimated spatial accuracies were well correlated, with an R-squared value of 0.936 ( $p < 0.001$ ). This analysis demonstrates good approximation of true spatial error using the standard model as employed in this study.

## **Supplemental Discussion**

### **Comparison of Sample Size with Prior Seminal Work**

The primary endpoint of the VMAP study evaluated regional accuracy in PVCs and VT without structural heart disease and ventricular scar burden  $< 10\%$ . In prior seminal work evaluating electrocardiographic imaging in PVCs and VT<sup>17</sup> without significant structural heart disease, 24 patients were enrolled. Electrocardiographic mapping successfully localized the arrhythmia origin to the right versus left ventricular outflow tracts in 23 of 24 patients (96%).

For comparison, the VMAP study enrolled 75 arrhythmia episodes for the primary endpoint. Regionalization accuracy was 98.7% (74 of 75 episodes). Overall, 53 ventricular arrhythmias originated from the outflow tracts in patients with and without structural heart disease; accuracy to identify left, right, or both ventricles in this group was 51/53 (96.2%).

In atrial arrhythmias, prior elegant work evaluated electrocardiographic imaging (ECGi) in 36 patients<sup>3</sup>. The distribution of patients included 7 during normal sinus rhythm, 3 during atrial pacing, and 26 with atrial fibrillation. Of the 26 patients with AF, 3 (12%) had AF during the ablation procedure which allowed assessment of the mechanistic relevance of mapped AF drivers with ablation.

In comparison, the VMAP study enrolled 118 atrial episodes, including 28 during atrial pacing and 21 during atrial fibrillation. Per the VMAP study protocol, all 21 AF patients were mapped during spontaneous or induced AF, and all (100%) either were non-inducible after ablation<sup>48</sup> or demonstrated a minimum of 6 months freedom from AF following the procedure<sup>28</sup>, providing mechanistic support for the relevance of identified “gold standard” sites.

In summary, VMAP study enrollment met pre-specified enrollment goals for all arrhythmias and pacing types and was comparable to prior seminal studies. Additional work is required to explore algorithm accuracy in larger populations.

### **Learning Set Composition and Comparison with Prior Work**

The machine learning set for this study consisted of  $> 1$  million arrhythmia simulations, which were organized into a reference “library” and leveraged for the mapping process. The simulation library was completed and “locked” before study initiation; no modifications to the library were permitted during the VMAP study protocol.

Other large data sets have been successfully employed in machine learning tasks. In prior work, Tison and colleagues used a large learning set to detect AF from smartwatch data in an ambulatory population<sup>49</sup>. Similarly, a learning set of monophasic action potential recordings<sup>50</sup> was used in prior work to derive novel insights and provide prognostic information regarding the risk for ventricular arrhythmias and sudden death.

Future studies are required to determine if additional simulations may be added to the algorithm library to improve accuracy or allow mapping in additional populations, such as complex congenital heart disease or dextrocardia.

### **Contributors to Mapping Accuracy**

Evaluation of study results suggests two main contributors to study mapping accuracy: a multitude of highly relevant computational simulations and robustness of the forward solution to assess and compare cardiac activation between patients and the computational models.

With respect to computational simulations, the VMAP study results demonstrate that accurate noninvasive mapping is possible using a forward solution approach which is not patient-specific but is instead highly patient-relevant because of user inputs to the mapping algorithm regarding the presence and location of diseased substrate. Future work is required to determine if accuracy can be further improved with additional input fields and additional computational sub-libraries for the mapping process.

Regarding the robustness of the forward-solution approach, we believe that analysis of cardiac depolarization as an integrated event provides the relative location of the arrhythmia source with respect to cardiac anatomical features (e.g., the intersection of the left ventricular free wall with the interventricular septum, the left ventricular apex, etc.) rather than a specific location in 3-dimensional space within the patient's body. Additionally, the results of the study support use of the Dower and Kors transformations to provide adequate detail for comparison with computational arrhythmia simulations. Finally, the mapping process is enhanced by redundancy<sup>51</sup> within the 12-lead ECG to cross-check the validity of recorded data. Additional investigations are required to determine whether alternatives to Dower and Kors transformations may provide greater accuracy for the mapping process.

## Supplemental Tables

**Supplemental Table I.** Feature mapped according to arrhythmia or pacing type.

<b>Arrhythmia/Pacing Type</b>	<b>Feature Mapped</b>
<b>Premature atrial complexes</b> <b>Premature ventricular complexes</b> <b>Focal atrial tachycardia</b> <b>Focal ventricular tachycardia</b> <b>Atrial pacing</b> <b>Ventricular pacing</b>	Site of early activation
<b>Orthodromic atrio-ventricular reentrant tachycardia</b>	Early atrial activation at accessory pathway insertion
<b>Macro-reentrant ventricular tachycardia</b>	Location of reentrant wavefront exit from protected isthmus
<b>Atrial fibrillation</b> <b>Ventricular fibrillation</b>	Areas of wavefront slowing and curvature, consistent with functional reentry electrical substrates



**Supplemental Table II.** Validation set results for primary and secondary endpoints.

Arrhythmia or Pacing Type	Regional Accuracy	Segmental Accuracy
Ventricular pacing	10 of 10 (100%)	10 of 10 (100%)
Ventricular fibrillation	10 of 10 (100%)	10 of 10 (100%)
Ventricular tachycardia	10 of 10 (100%)	10 of 10 (100%)
Premature ventricular complex	9 of 10 (90%)	8 of 10 (80%)
Atrial pacing	12 of 12 (100%)	12 of 12 (100%)
Atrial fibrillation	18 of 19 (94%)	18 of 19 (94%)
Atrial tachycardia	11 of 11 (100%)	11 of 11 (100%)
Premature atrial complex	10 of 10 (100%)	9 of 10 (90%)
Atrioventricular re-entrant tachycardia	10 of 10 (100%)	10 of 10 (100%)
<b>Overall</b>	<b>100 of 102 (98%)</b>	<b>98 of 102 (96%)</b>

**Supplemental Table III: Primary Endpoint Analysis by Center.**

Agreement	Investigational Site (Site Number)				
	UCSD (01)	VA San Diego (02)	Sutter Health (03)	MUSC (04)	TOTAL
Total Episodes* [n (%)]	41 (54.7%)	17 (22.7%)	6 (8.0%)	11 (14.7%)	75 (100%)
Agreement	41 (100%)	17 (100%)	5 (83.3%)	11 (100%)	74 (98.7%) <sup>†</sup>
No Agreement <sup>‡</sup>	0 (0.0%)	0 (0.0%)	1 (16.7%)	0 (0.0%)	1 (1.3%)

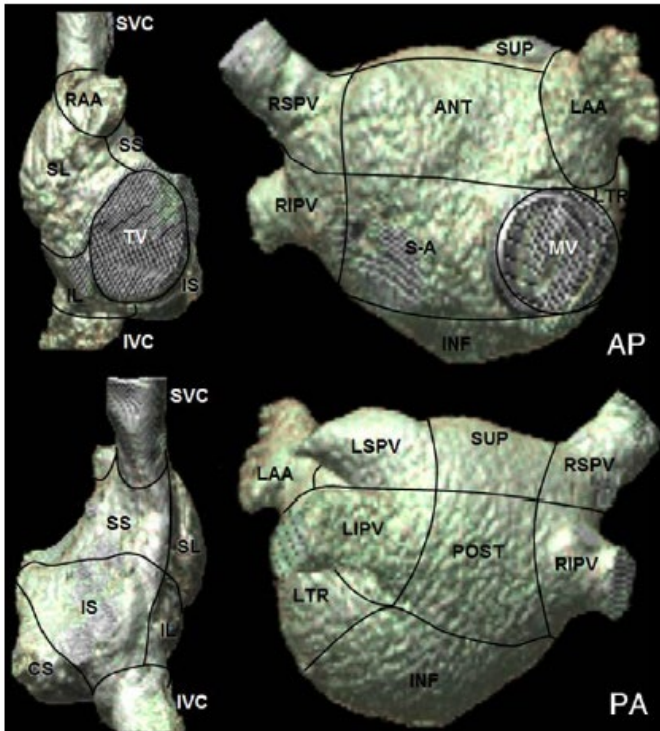
\*Only episodes that met the primary endpoint population criteria were included in the primary endpoint analysis.

<sup>†</sup>Primary endpoint ( $p < 0.0001$  to reject pre-specified null hypothesis, CI: [96.0% - 99.9%]).

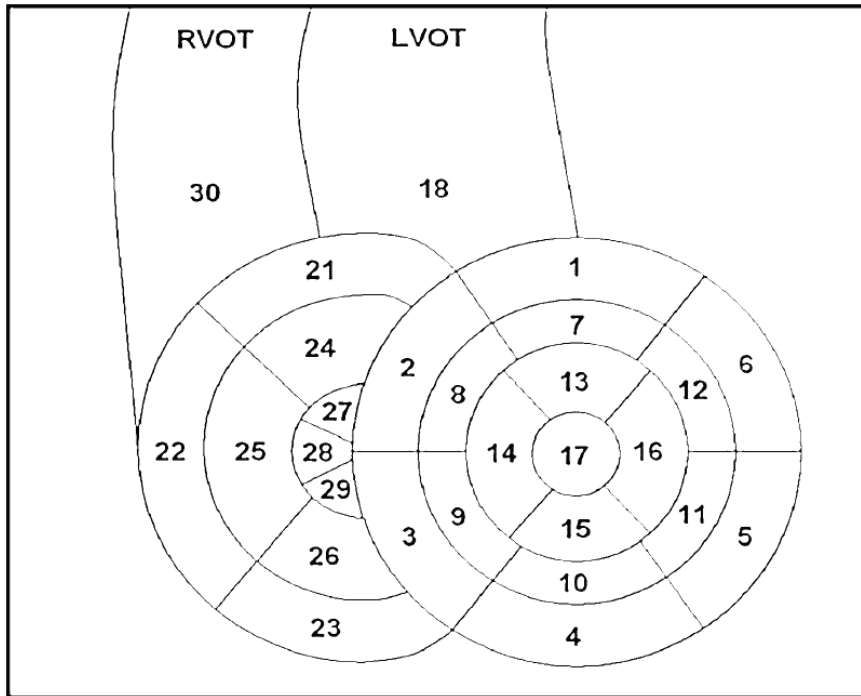
<sup>‡</sup>Fisher's exact test for difference in accuracy between investigational sites:  $p = 0.08$  (differences not statistically significant).

Key: UCSD = University of California San Diego, VA San Diego = Veterans Affairs San Diego Medical Center, MUSC = Medical University of South Carolina

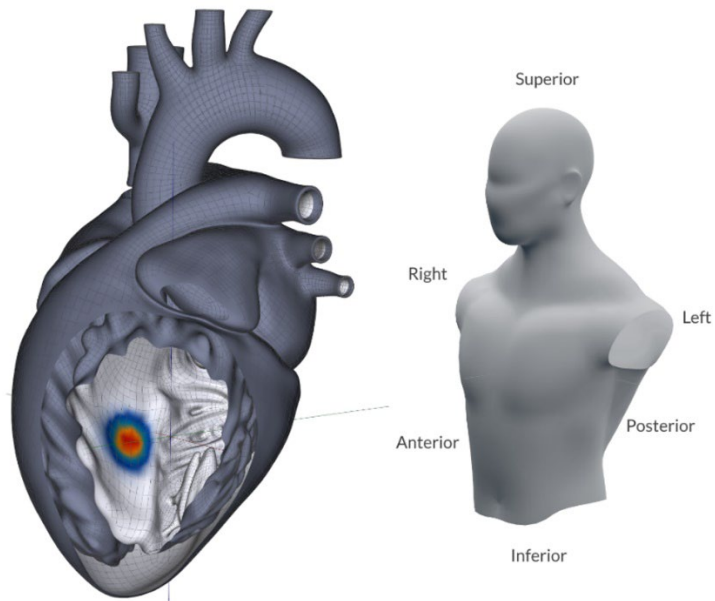
## Supplemental Figures and Figure Legends



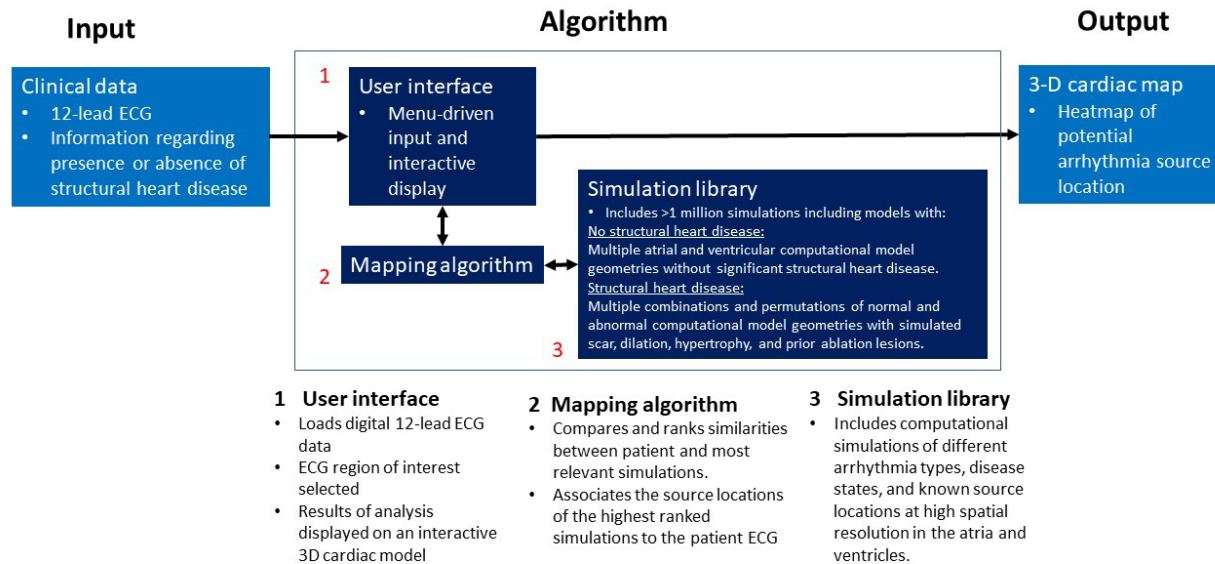
**Supplemental Figure I. Pre-defined atrial segments.** Three-dimensional reconstruction from preprocedural cardiovascular magnetic resonance imaging of the right (RA) and left atrium (LA) in anterior/posterior (AP) and posterior/anterior (PA) view. The RA was divided into the following segments: right atrial appendage (RA RAA), coronary sinus ostial area (RA CS), superior lateral (RA SUP LAT), inferior lateral (RA INF LAT), superior septal (RA SUP SEP), inferior septal (RA INF SEP), superior cava vein (SCV), and inferior cava vein (ICV). The LA was divided into the following segments: superior (LA SUP), posterior (LA POST), anterior (LA ANT), inferior (LA INF), lateral (LA LAT), right superior pulmonary vein (LA RSPV), right inferior PV (LA RIPV), left superior PV (LA LSPV), left inferior PV (LA IPV), septal-anterior (LA SEPT ANT), left atrial appendage (LAA), mitral valve (MV) annulus, and tricuspid valve (TV) annulus. Figure from Sohns et al<sup>12</sup> reprinted with permission.



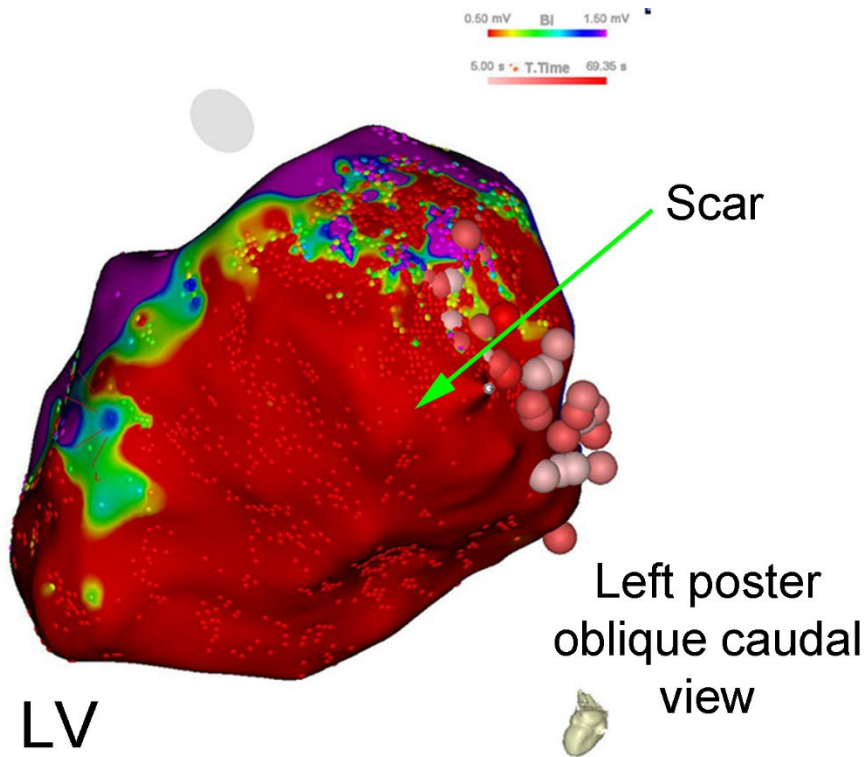
**Supplemental Figure II. Pre-defined ventricular segments.** Segmental division of the right ventricle, outflow tracts, and other structures to supplement the 17 segment American Heart Association left ventricular segmentation model. Numbers 19 and 20 (not shown) were defined as the left ventricular papillary muscles and right ventricular moderator band. Figure from Plaisier et al<sup>13</sup> reprinted under a Creative Commons license from Springer Nature. Key: RVOT = right ventricular outflow tract, LVOT = left ventricular outflow tract.



**Supplemental Figure III: Arrhythmia simulation library sample.** A simulation library sample consists of an arrhythmia simulation, initiated at a source (red marker) determined by input parameters. In this example, the arrhythmia source is located at the interventricular septum (cutaway model).

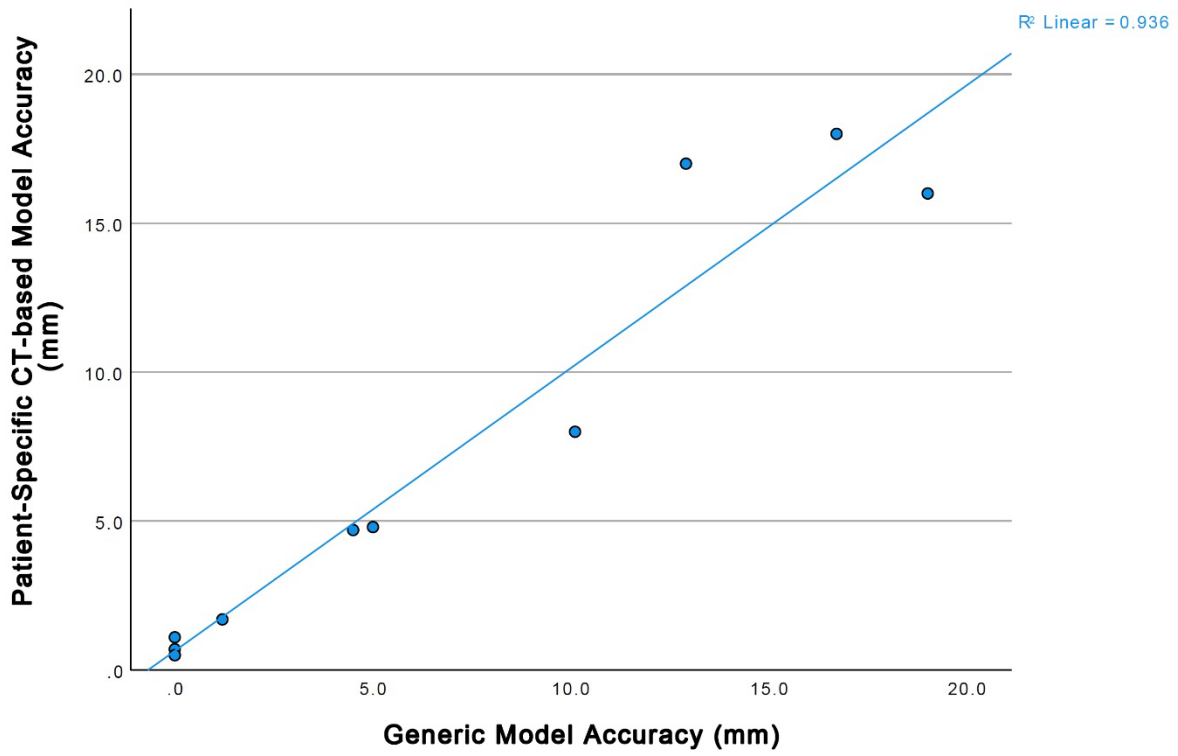


**Supplemental Figure IV. VMAP Study: Algorithm Inputs, Processes, and Outputs.**



**Supplemental Figure V.** Voltage map for study patient during VT ablation, corresponding to patient illustrated in manuscript Figure 2, second row. This left posterior oblique, caudal view demonstrates a large inferior/posterior scar. Colors represent endocardial bipolar voltage, with red regions exhibiting voltages less than 0.5 mV (scar) and purple regions greater than 1.5 mV (normal myocardium).

**Patient-Specific CT-based Model Accuracy (mm) by Generic Model Accuracy (mm)**



**Supplemental Figure VI.** Modeled vs true spatial accuracy in a subset of patients from the VMAP study.